Supplement of Weather Clim. Dynam., 4, 471–487, 2023
https://doi.org/10.5194/wcd-4-471-2023-supplement

Supplement of

The teleconnection of extreme El Niño–Southern Oscillation (ENSO) events to the tropical North Atlantic in coupled climate models

Jake W. Casselman et al.

Correspondence to: Jake William Casselman (cjake@ethz.ch)

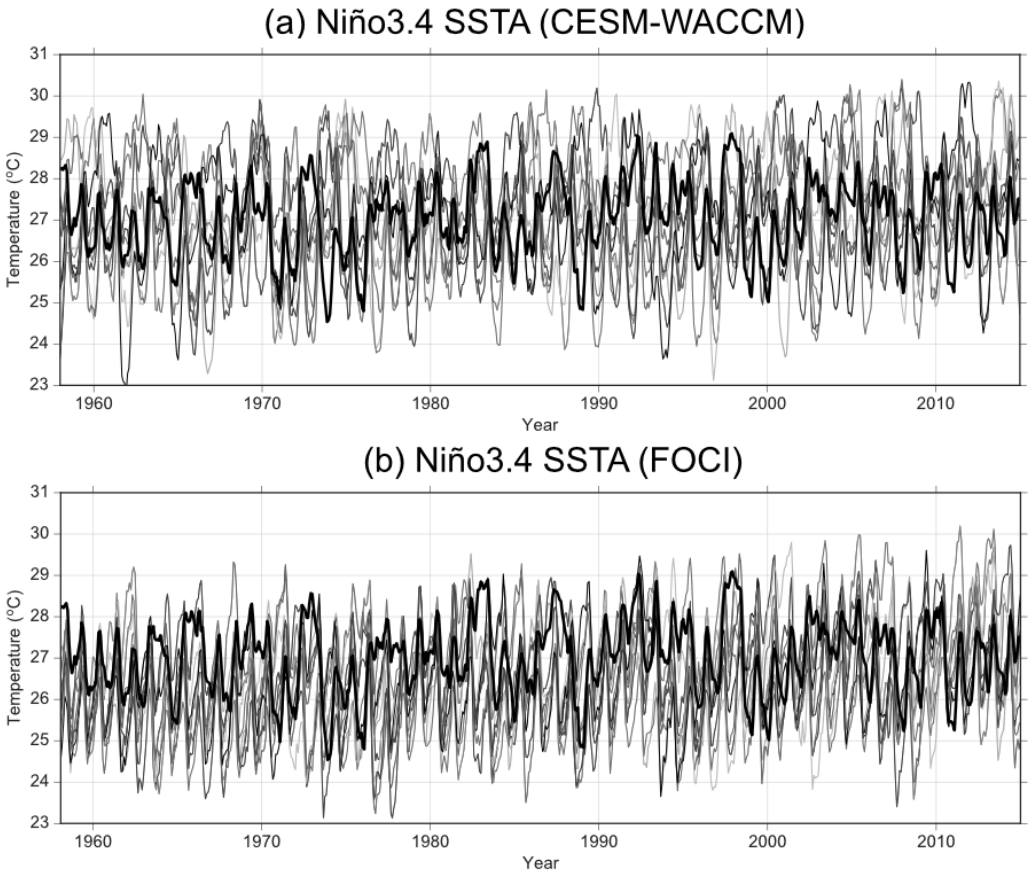

Figure S1: Comparison of individual ensemble members for CESM-WACCM (a), and FOCI (b) with reanalysis. The timeseries have not been detrended. The bold black line represents the ERSSTv5 from 1958 until 2014, while the grey lines represent the different model ensemble members.

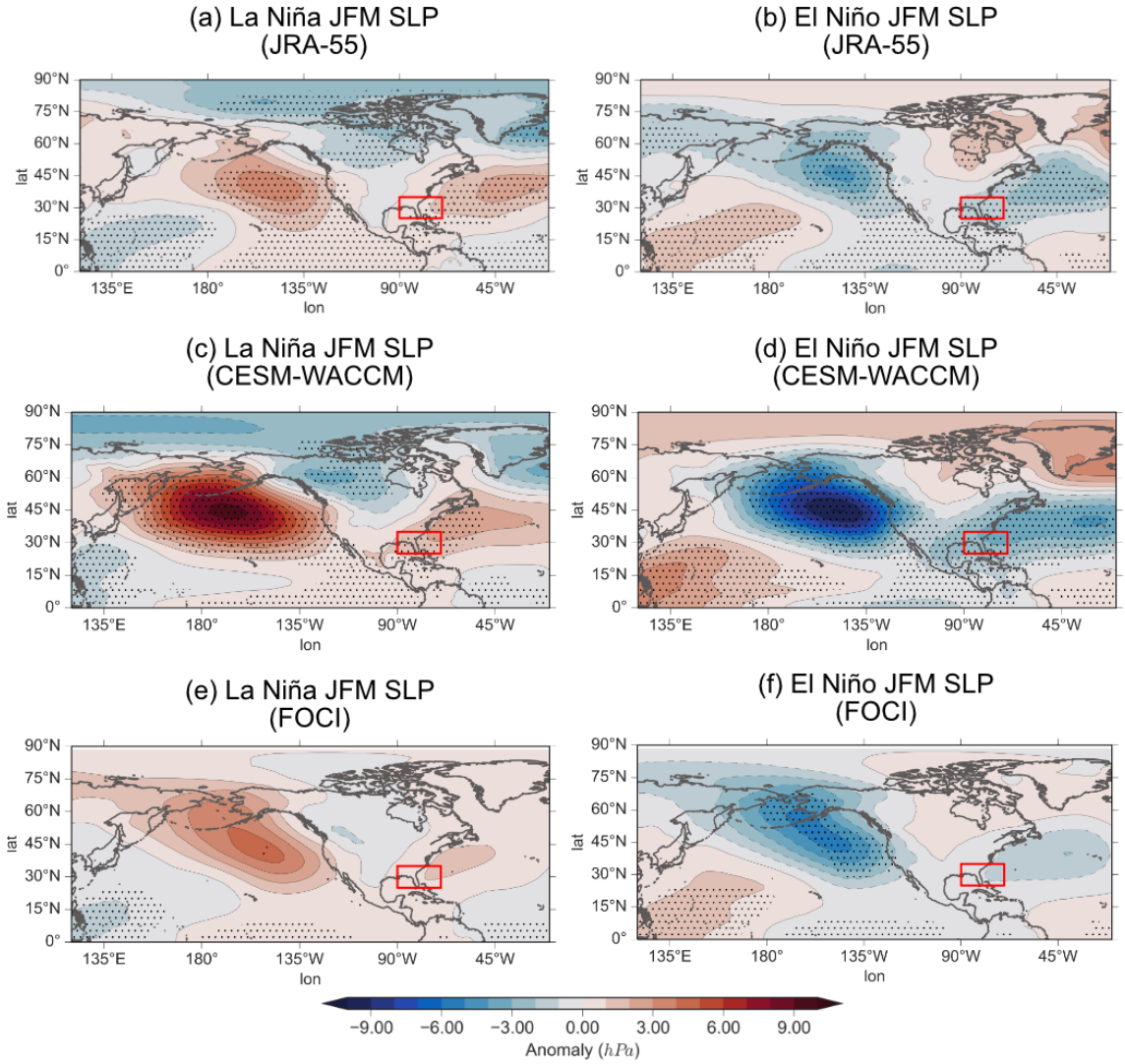

Figure S2: Mean sea level pressure composites in JFM following a strong (1-2 std dev) ENSO event (left is La Niña, right is El Niño). The response from JRA-55, CESM, and FOCI are represented in panels a-b, c-d, and e-f, respectively. Stippling represents areas that are statistically significant from zero at the 95% level, and the red box indicates the area used for the Southeastern low index.

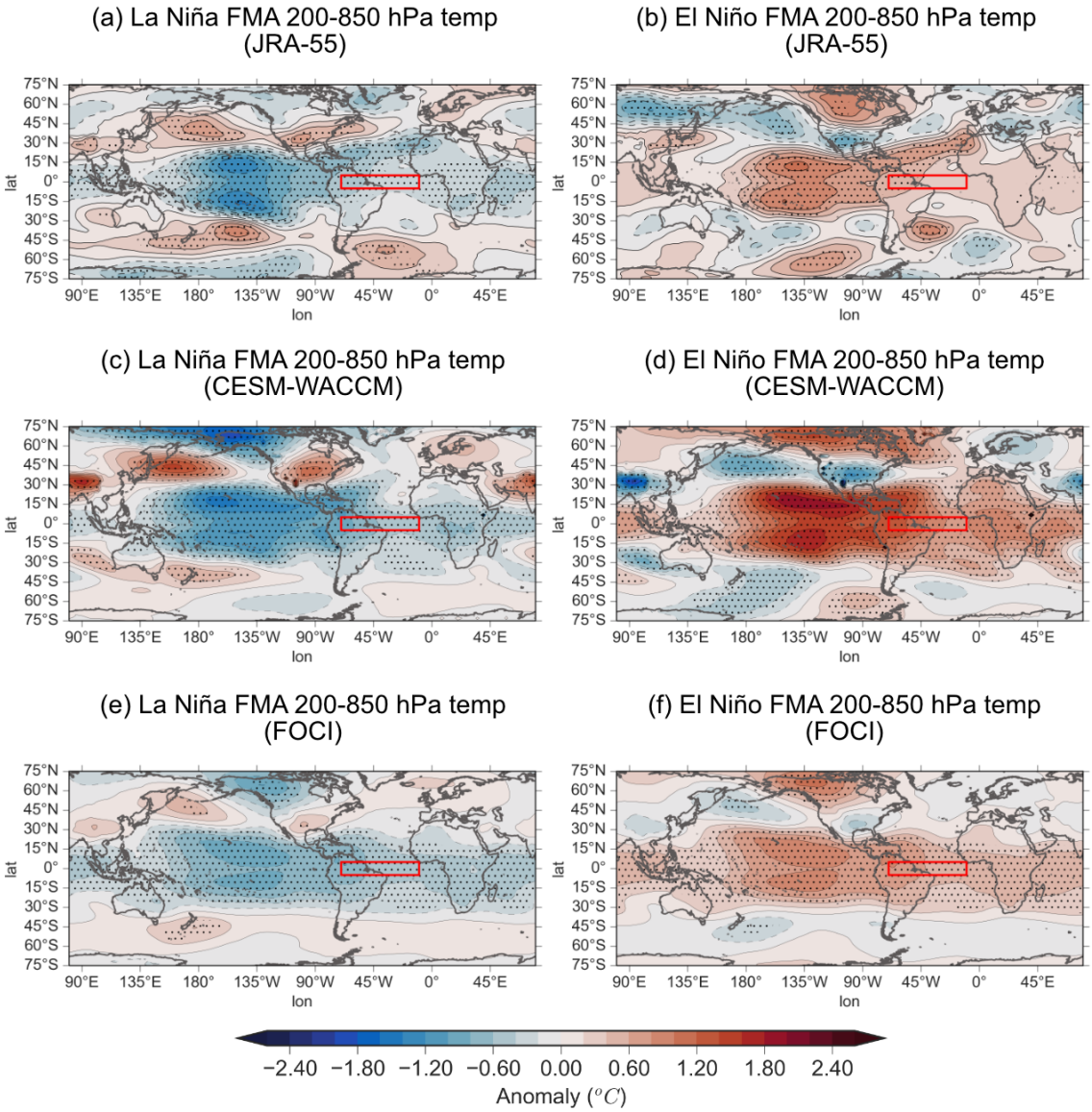

Figure S3: Mean tropospheric temperature averaged from 850 to 200 hPa in FMA following a strong (1-2 std dev) ENSO event (left is La Niña, right is El Niño). The response from JRA-55, CESM, and FOCI are represented in panels a-b, c-d, and e-f, respectively. Stippling represents areas that are statistically significantly different from zero at the 95% level, and the red box indicates the area used for the Tropospheric Temperature index.

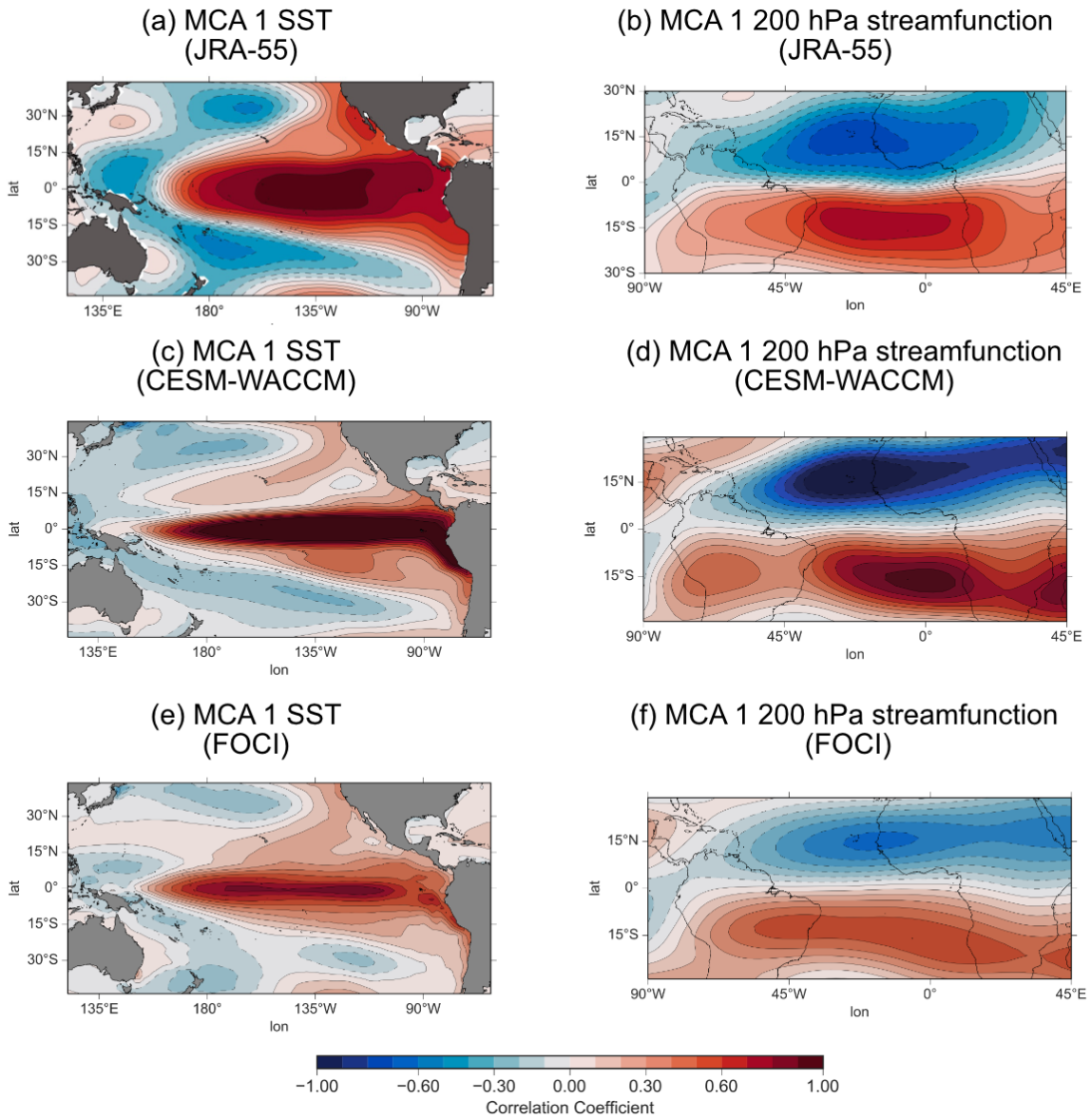

Figure S4: Comparison of Maximum Covariance Analysis (MCA) 1 between the SST over the Pacific and (left) and 200 hPa streamfunction over the tropical Atlantic (right). The response from JRA-55, CESM, and FOCI are represented in panels a-b, c-d, and e-f, respectively. Each model's MCA response is averaged across the ensemble to provide an average response.

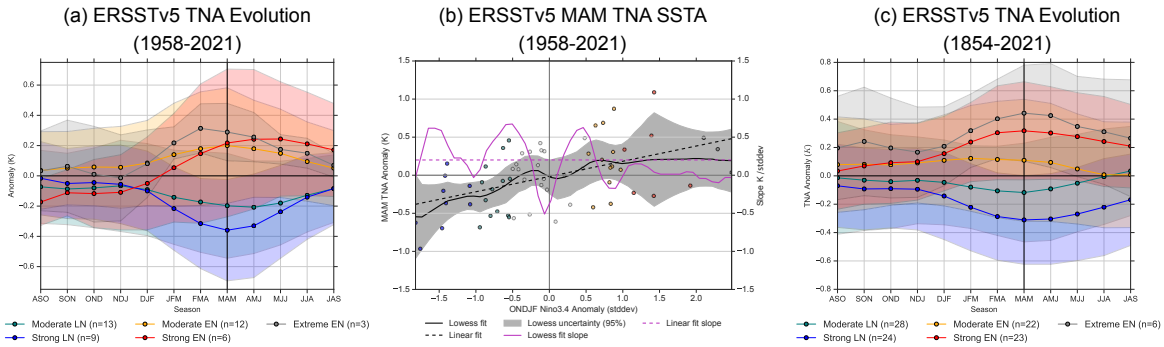

Figure S5: The figure displays the composited 3-month seasonal evolution of the TNA SSTA (1958-2021, in K) (a), the MAM TNA SSTA vs. the previous ONDJF Niño3.4 index (b) (see Figure 1a-b in the manuscript for comparison), and the composited extended 3-month seasonal evolution of the TNA SSTA (1854-2021, in K) (c). In panel (b), the LOWESS curve is shown in solid black, and the 95% confidence interval for the LOWESS curve is represented by shading. The linear fit is depicted by the dashed line. The LOWESS curve is created using bootstrapping and resampling (with replacement) 1000 times. The methods employed follow Casselman et al., 2021.

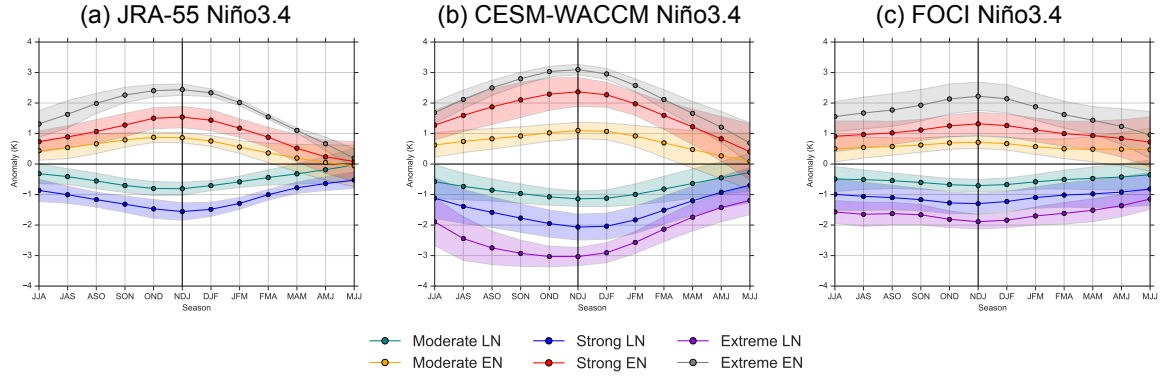

Figure S6: Composited 3-month average seasonal evolution of the Niño3.4 SSTA (in K) for JRA-55 (a, 1958-2021) and the ensemble means for CESM-WACCM (b), and FOCI (c). Events are subsampled into moderate, strong, and extreme events, as outlined in the methods. Shading represents the 95% confidence interval, while the solid line represents the mean.

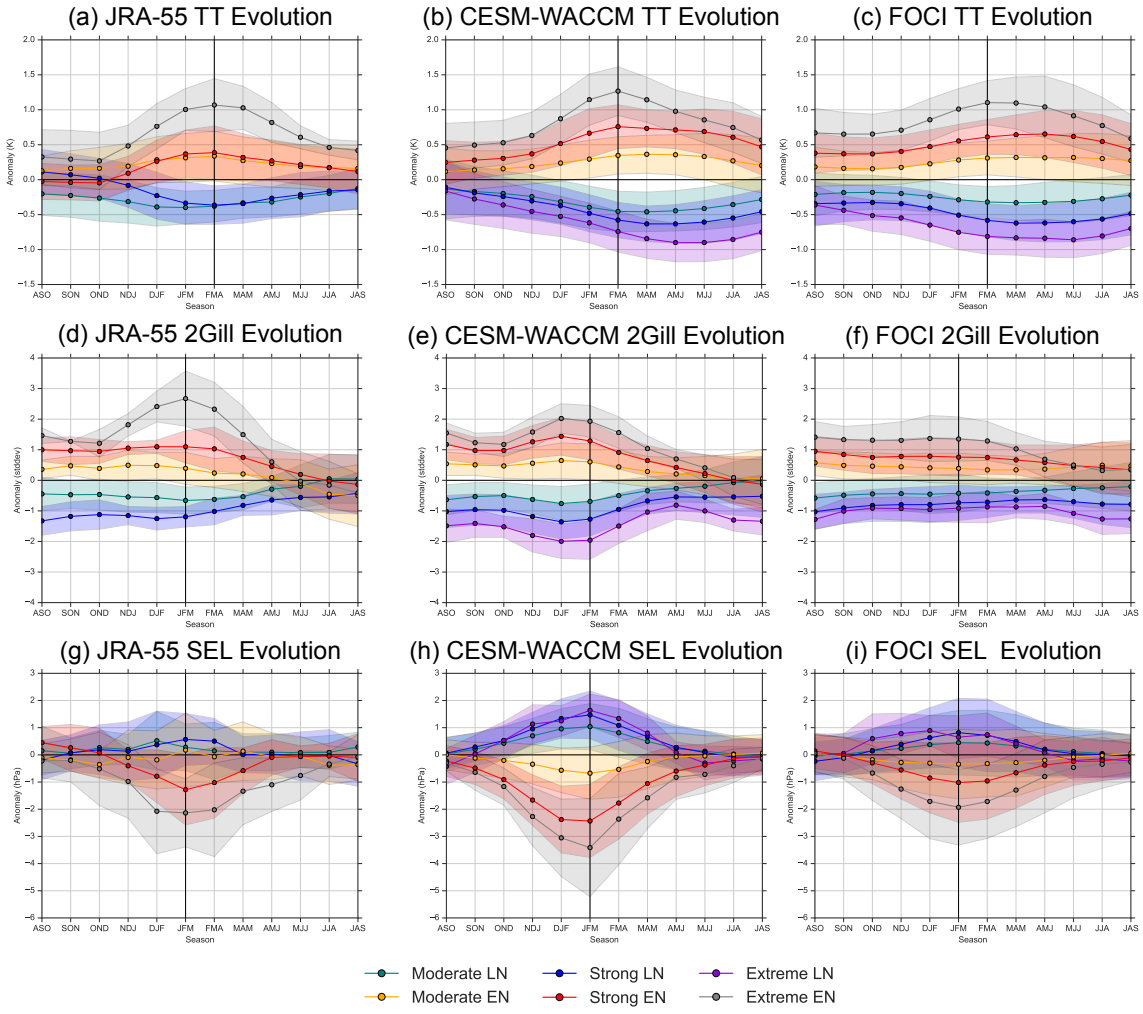

Figure S7: Similar to Supplementary Figure S6, except for the TT (top), Secondary Gill (2Gill, middle), and Southeastern Low (SEL, bottom) indices.

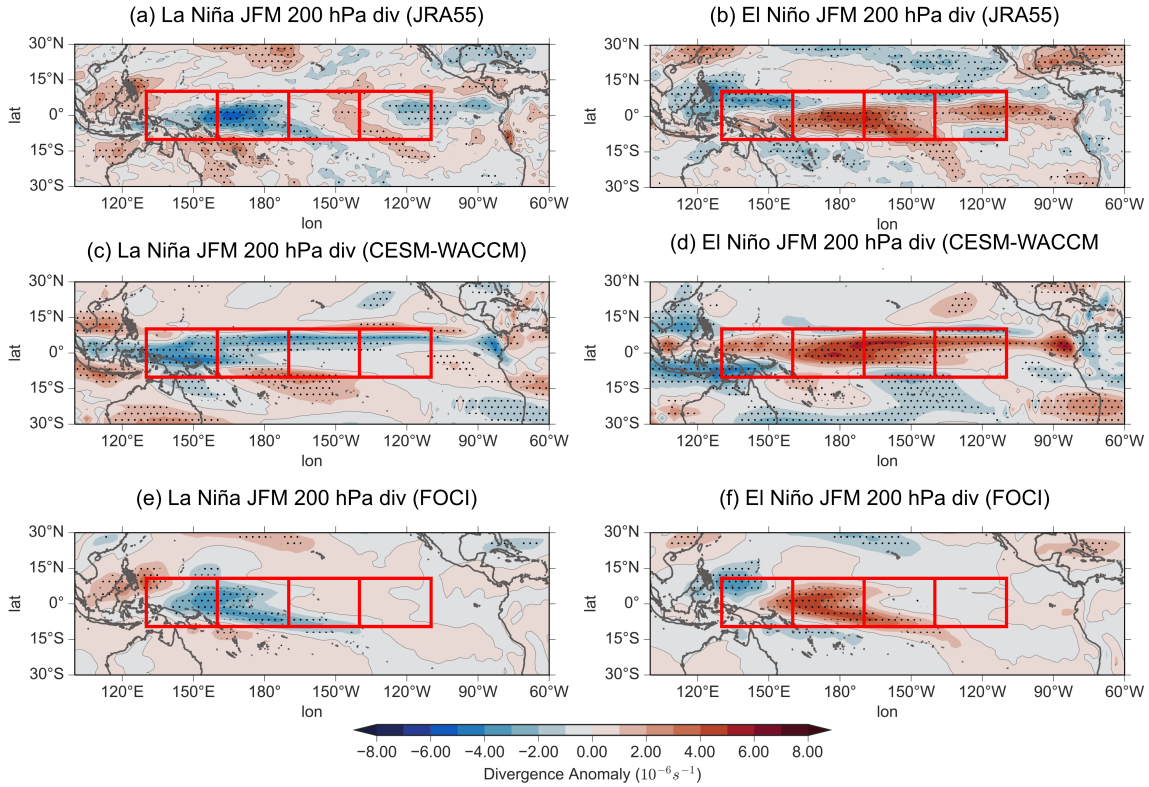

Figure S8: 200 hPa JFM divergence composites over the tropical Pacific following a strong (1-2 std dev) ENSO event (left is La Niña, right is El Niño). The response from JRA-55, CESM, and FOCI are represented in panels a-b, c-d, and e-f, respectively. Stippling represents areas that are statistically significantly different from zero at the 95% level, and red boxes show the divergence areas used in figure S9.

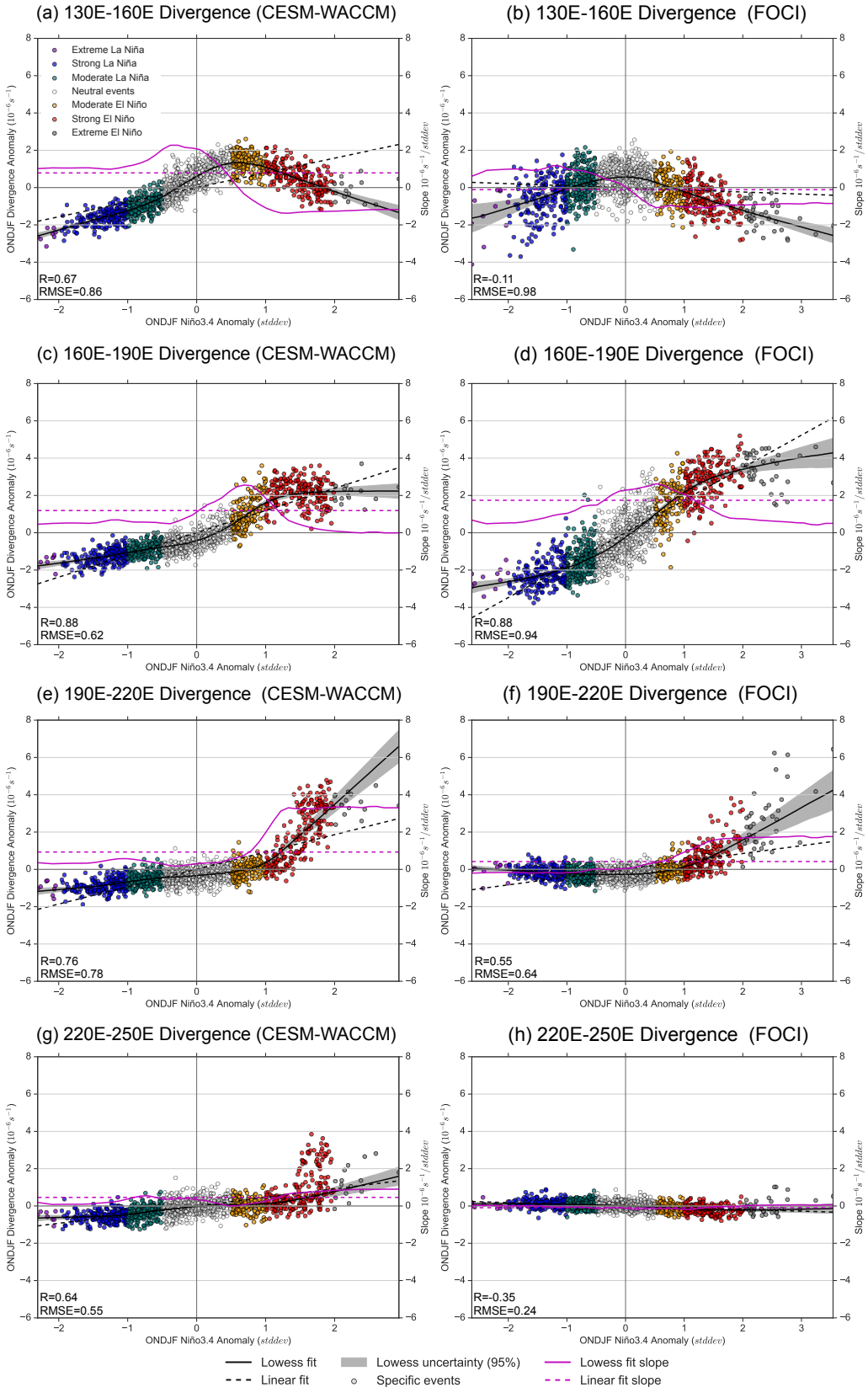

Figure S9: Relationship between the ONDJF Niño3.4 SSTA and ONDJF 200 hPa divergence over the Pacific. The divergence is averaged between 10°S-10°N, and varies between 130°E and 110°W (with 30° steps). The scatter plot uses the same color scheme as presented in Supplementary Figure S5.

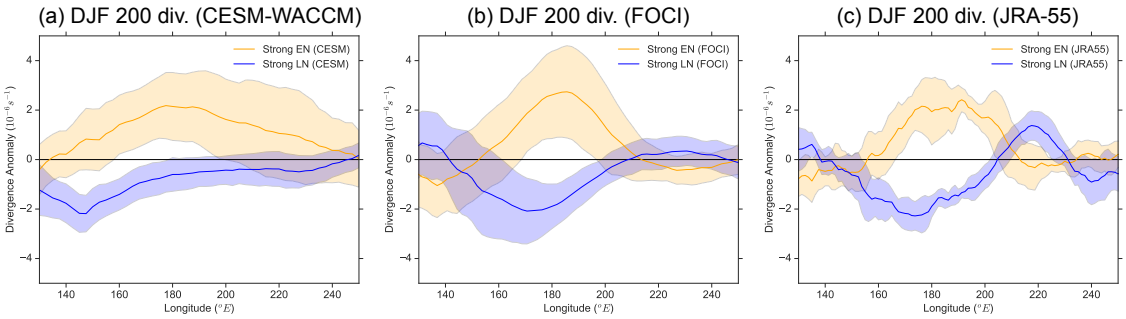

Figure S10: Divergence analysis over the tropical Pacific (averaged between 10°N-10°S) following an ENSO event. Panels a-c show the relationship between the ONDJF Niño3.4 SSTA and DJF 200 hPa divergence over the Pacific for CESM-WACCM (a), FOCI (b) and JRA-55 (c). Divergence is averaged between 10°S-10°N, and subsampled for strong events only (1-2 std dev), and shading represents ±1.0 std dev.

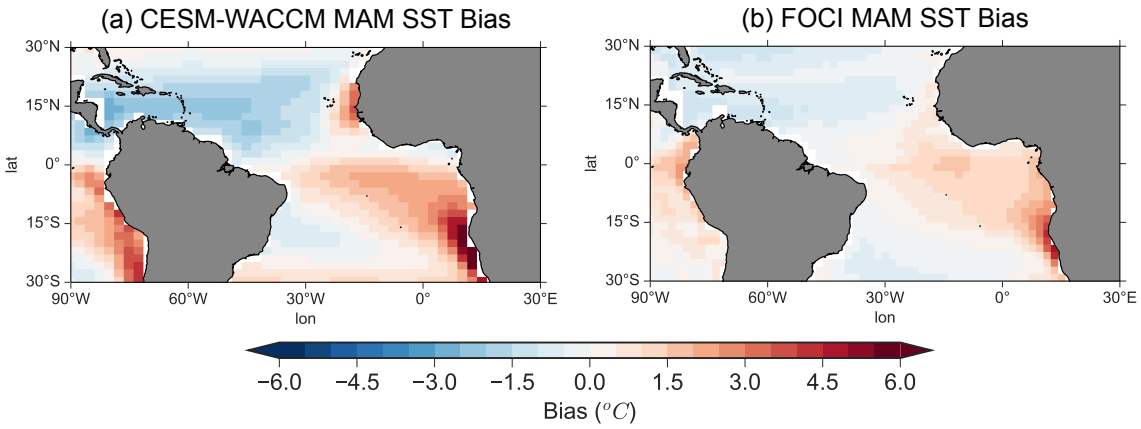

Figure S11: CESM-WACCM (left) and FOCI (right) SST bias with respect to ERSSTv5, with all datasets averaged from 1958 to 2014. ERSST is interpolated to the grid of the given model, and the tropical (30°N-30°S) mean SSTs are removed from all datasets before computing the difference (model average minus ERSSTv5).

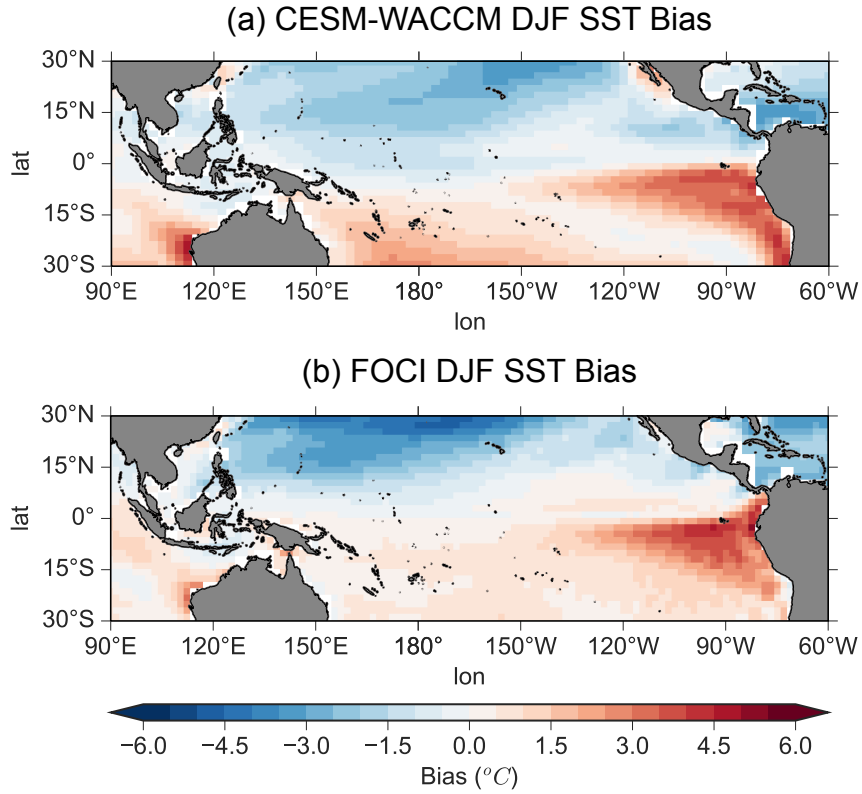

Figure S12: CESM-WACCM (left) and FOCI (right) SST bias with respect to ERSSTv5 using the same method as S11, except over the Pacific and averaged for December-February (DJF) instead.

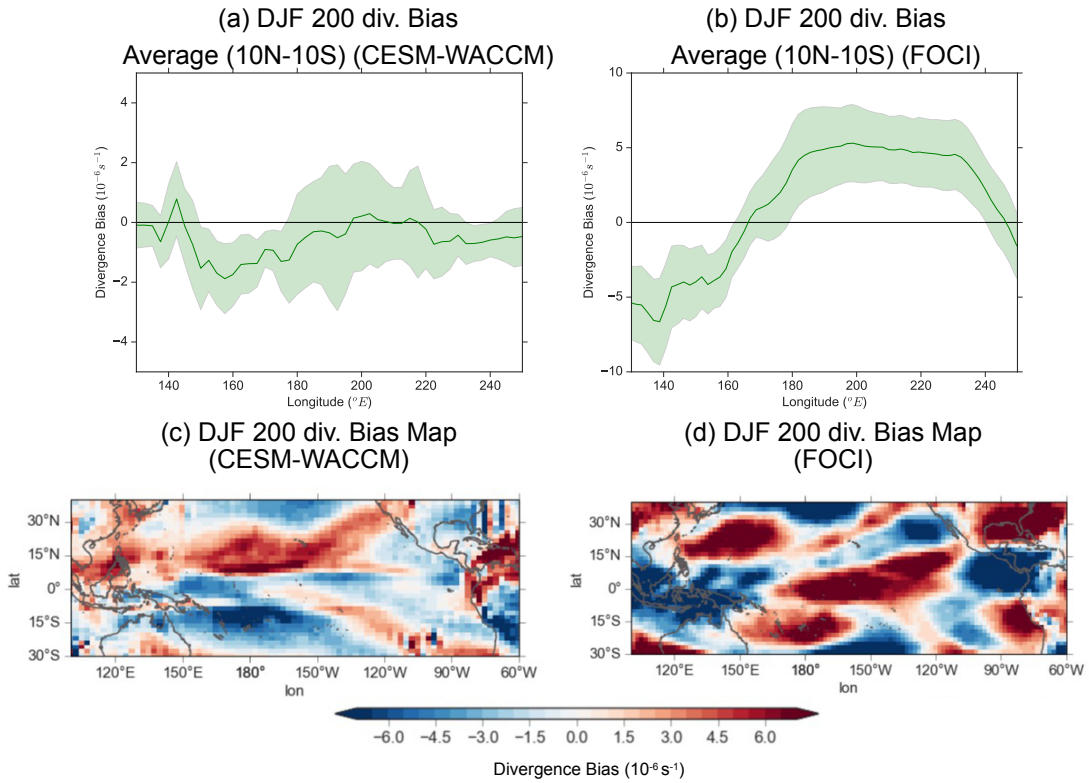

Figure S13: Divergence analysis over the tropical Pacific for background climatology biases. Panels a-b show DJF 200 hPa divergence bias averaged between 10°N-10°S with respect to JRA-55, while panels c-d show the spatial pattern for DJF 200 hPa divergence bias with respect to JRA-55. All datasets averaged between 1958 and 2014.